

Accepted Manuscript

Potassium Channel Blocking 1,2-Bis(aryl)ethane-1,2-diamines Active as Antiarrhythmic Agents

Johan Kajanus, Thomas Antonsson, Leif Carlsson, Ulrik Jurva, Anna Pettersen, Johan Sundell, Tord Inghardt

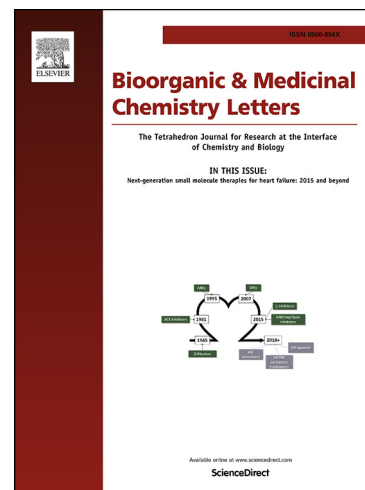
PII: S0960-894X(19)30136-2
DOI: <https://doi.org/10.1016/j.bmcl.2019.03.006>
Reference: BMCL 26320

To appear in: *Bioorganic & Medicinal Chemistry Letters*

Received Date: 17 December 2018
Revised Date: 19 February 2019
Accepted Date: 5 March 2019

Please cite this article as: Kajanus, J., Antonsson, T., Carlsson, L., Jurva, U., Pettersen, A., Sundell, J., Inghardt, T., Potassium Channel Blocking 1,2-Bis(aryl)ethane-1,2-diamines Active as Antiarrhythmic Agents, *Bioorganic & Medicinal Chemistry Letters* (2019), doi: <https://doi.org/10.1016/j.bmcl.2019.03.006>

This is a PDF file of an unedited manuscript that has been accepted for publication. As a service to our customers we are providing this early version of the manuscript. The manuscript will undergo copyediting, typesetting, and review of the resulting proof before it is published in its final form. Please note that during the production process errors may be discovered which could affect the content, and all legal disclaimers that apply to the journal pertain.

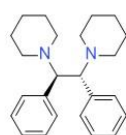


Graphical Abstract

Potassium Channel Blocking 1,2-Bis(aryl)ethane-1,2-diamines Active as Antiarrhythmic Agents

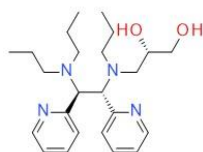
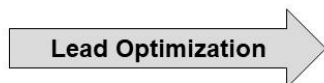
Leave this area blank for abstract info.

Johan Kajanus, Thomas Antonsson, Leif Carlsson, Ulrik Jurva, Anna Pettersen, Johan Sundell and Tord Inghardt



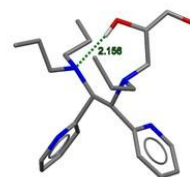
1

CYP2D6 inhibition
Poor selectivity vs IKs
DDI risk (CYP3A4 only)
Reactive metabolites



10

Clean CYP profile
Inactive at IKs
Several routes of elimination
No reactive metabolites





Potassium Channel Blocking 1,2-Bis(aryl)ethane-1,2-diamines Active as Antiarrhythmic Agents

Johan Kajanus^{a*}, Thomas Antonsson^a, Leif Carlsson^a, Ulrik Jurva^a, Anna Pettersen^b, Johan Sundell^a and Tord Inghardt^{a*}

^a Cardiovascular, Renal and Metabolism, IMED Biotech Unit, AstraZeneca, Gothenburg, Sweden

^b Pharmaceutical Sciences, IMED Biotech Unit, AstraZeneca, Gothenburg, Sweden

ARTICLE INFO

Article history:

Received

Revised

Accepted

Available online

Keywords:

Kv1.5

IK_{ur}

Atrial fibrillation

Antiarrhythmic agents

Potassium channel blocker

1,2-Bis(aryl)ethane-1,2-diamines

ABSTRACT

Atrial fibrillation (AF) is a major cause of stroke, heart failure, sudden death and cardiovascular morbidity. The Kv1.5 potassium channel conducts the I_{Kur} current and has been demonstrated to be predominantly expressed in atrial versus ventricular tissue. Blockade of Kv1.5 has been proven to be an effective approach to restoring and maintaining sinus rhythm—in preclinical models of AF. In the clinical setting, however, the therapeutic value of this approach remains an open question. Herein, we present synthesis and optimization of a novel series of 1,2-bis(aryl)ethane-1,2-diamines with selectivity for Kv1.5 over other potassium ion channels. The effective refractory period in the right atrium (RAERP) in a rabbit PD model was investigated for a selection of potent and selective compounds with balanced DMPK properties. The most advanced compound (**10**) showed nanomolar potency in blocking Kv1.5 in human atrial myocytes and based on the PD data, the estimated dose to man is 700 mg/day. As previously reported, **10** efficiently converted AF to sinus rhythm in a dog disease model.

2018 Elsevier Ltd. All rights reserved.

* Johan Kajanus. Tel.: +46-31-7762812; e-mail: johan.kajanus@astrazeneca.com

* Tord Inghardt. Tel.: +46-31-7761954; e-mail: tord.inghardt@astrazeneca.com

Although the management of patients with atrial fibrillation (AF) has advanced in recent years, this arrhythmia remains one of the major causes of stroke, heart failure, sudden death, and cardiovascular morbidity in the world. It affects approximately 2% of the general population, increasing to more than 10% at ages above 80.¹ Two major treatment strategies prevail: prevention of stroke through the use of anticoagulants; and antiarrhythmic approaches which strive towards restoring sinus rhythm or controlling heart rate. Atrial fibrillation is a progressive disease resulting in atrial electrophysiological change and structural remodeling which promotes AF itself and eventually results with AF being permanent.^{2,3} The presently available pharmacological options for AF management have limited efficacy and are associated with considerable risks, particularly proarrhythmia.² Attractive prospects for improved AF management include drugs that selectively target ion channels such as the ultra-rapidly activating outward potassium current (IKur), the acetylcholine-activated inwardly directed potassium current (IKAch), and the small conductance Ca²⁺-activated (SK) potassium channels engaged in atrial repolarization.^{2,4} Such atrial repolarization-delaying agents would, at least theoretically, increase atrial refractoriness and consequently restore and maintain normal sinus rhythm without the undesired effects of impulse propagation and cardiac contractility and circumvent ventricular proarrhythmia liability. However, few such agents are currently in clinical use or under clinical investigation. Vernakalant is approved for conversion of recent onset AF and is considered to block atrial early repolarizing currents including IKur. AZD2929 and NTC-801 (BMS-914392) are investigational agents which selectively block IKACh though they failed to demonstrate anticipated electrophysiological action and antiarrhythmic efficacy in early clinical studies.^{3,5}

Of the potentially atrial-selective currents, IKur has been the target for the most intensive research efforts and the first to raise attention.³ The Kv1.5 potassium channel conducts the human IKur and has been demonstrated to be predominantly expressed in human atrial versus ventricular tissue. This observation is supported by the absence of the IKur current in human ventricular cardiomyocytes and the failure of potent, selective IKur blockers to prolong ventricular action potential duration *in vitro* and delay ventricular repolarization *in vivo*.^{3,6} Taken together, these experimental findings provide compelling evidence of IKur as an atrial-selective target. Considerable resources have been invested in identifying and developing efficacious and safe IKur blockers of various chemical classes (Chart 1).⁷⁻⁹ However, despite convincing experimental data, whether the Kv1.5 channel is an effective target for antiarrhythmic therapy in the clinical setting is still an open question. That XEN-D0103, a selective Kv1.5 blocker in early clinical testing, failed to reduce AF burden in patients with paroxysmal AF adds to the uncertainty.¹⁰

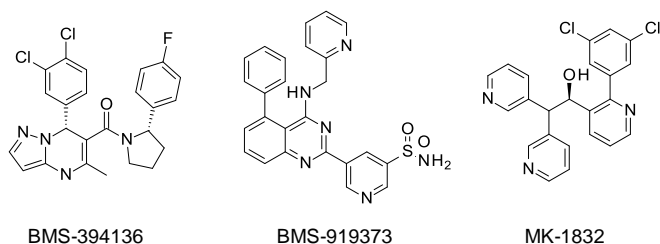


Chart 1. Representative examples of Kv1.5 blockers from different chemical series.

We have previously reported on our efforts to develop Kv1.5 inhibitors based on diphenylphosphine amides and oxides (resembling the diphenylphosphine oxide DPO-1¹¹),¹² lactam sulfonamides,¹³ and isoindolinones¹⁴ (Chart 2). In this report, we present our work on a series of 1,2-bis(aryl)ethane-1,2-diamines.

Compd	Kv1.5 IC ₅₀ ^a (μM)	hERG IC ₅₀ ^b (μM)	IKs IC ₅₀ (μM)	CYP2D6 IC ₅₀ ^b (μM)	LogD ^c	CLint (μl/min/mg)	HLM
1	0.41	>33	1.4	0.13	4.0	14	
2	2.2	>33	17	>20	2.2	<5	
3	0.22 ^b	6.3	>33 ^b	>20	4.6	58 ^b	
4	3.2	>33	60	5.4	3.3	23	

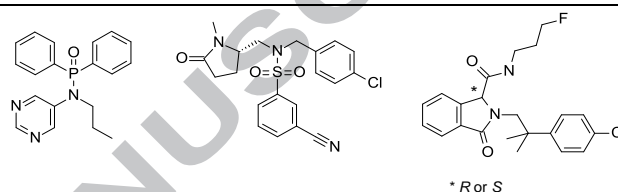
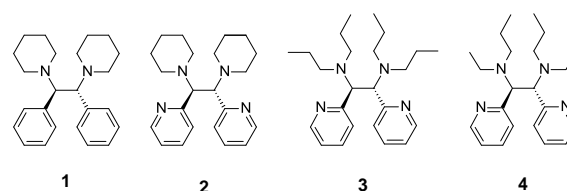


Chart 2. Examples of Kv1.5 blockers from previous AstraZeneca series.

The present series originated from a focused screen of the AstraZeneca corporate compound collection in which a virtual screen was performed with both in-house and competitor compounds as seeds. A hit from this screen was the symmetrical diamine **1** (Table 1), which docked very nicely into a homology model of Kv1.5, and was a promising starting point for further optimisation.¹⁵ The compound was potent *in vitro* and showed excellent potency in an initial *in vivo* mouse PD model which utilized the QT interval as a surrogate marker for blockade of the Kv1.5 channel, thus giving low predicted doses to man. However, the compound was a strong CYP2D6 inhibitor, gave rise to reactive metabolites (tested by cyanide trapping of iminium ions) and was found to be a blocker of the IKs current.

Replacing the phenyl rings in **1** with 2-substituted pyridyl rings, giving **2**, markedly lowered the CYP2D6 and IKs inhibition, which partly may be explained by the lowering of logD. However, with *N*-alkyl chain analogs like **3**, CYP2D6 and IKs inhibition was still maintained at a low level despite a higher logD. Furthermore, the issue with reactive metabolites, caused by iminium ion formation, was decreased when cyclic amines were replaced with acyclic *N*-alkyl groups. Finally, compound **4**, the acyclic analog of **2**, was found to be potent on Kv1.5 and gratifyingly also selective against hERG and IKs. The compound was also found to be reasonably metabolically stable in human liver microsomes and did not give rise to any reactive metabolites (*e.g.* iminium ion formation).

Table 1. From hit to a selective lead compound



Values represent average of 2 measurements unless otherwise noted.

^a Assayed using IonWorks™ HT technology in CHO cells.¹⁶

^b n=1

^c Lipophilicity measured by chromatography.¹⁷

A feature that was found among the symmetrically substituted molecules like **1-4** was that the *meso* compound (*S,R*) displayed much higher lipophilicity than the two enantiomers (*R,R*) and (*S,S*). Compounds **2** (*S,S*-isomer), **5** (*meso*) and **6** (*R,R*-isomer) illustrate this point with measured logD values (Table 2) of 2.2, 4.6 and 2.2, respectively, a consequence of the differences in pKa (10.4 for the enantiomers and 8.7 for the *meso* compound). There is also a large difference in metabolic stability of these compounds, where **2** and **6** are metabolically stable and **5** is highly cleared. We hypothesize that the difference in pKa and other properties relate to the ability of the compounds to bind a proton using both amine nitrogens. In the chiral compounds, this can be accomplished with the two amine nitrogens in the same, or nearly the same plane, without steric clash of the two neighbouring aryl groups (Table 2). The same way of binding is less favorable in the *meso* compound **5** where the two aryl groups are eclipsed, which results in a sterically unfavorable interaction, hence, basicity is significantly reduced.

Table 2. Importance of relative stereochemistry



Compound	Kv1.5 IC ₅₀ (μM) ^a	LogD ^c	CLint HLM (μl/min/mg)	pKa
2	2.2	2.2	<5	10.4
5	1.4 ^b	4.6	412	8.7
6	4.8	2.2	<5	10.4

Values represent average of 2 measurements unless otherwise noted.

^a Assayed using IonWorks™ HT technology in CHO cells.¹⁶

^b n=1

^c Lipophilicity measured by chromatography.¹⁷

We found that compounds **1-6** were nearly exclusively metabolized by CYP3A4 and would therefore be very sensitive to drug-drug interactions (DDI), *i.e.* that co-administration with a potent inhibitor of CYP3A4 could increase circulating levels of compounds **1-6** and decrease margins to safety related findings, or that co-administration with a strong inducer of CYP3A4 could reduce exposure below the desired therapeutic level.¹⁸ With a view to mitigate this risk, we decided next to investigate introduction of functional groups with the potential to undergo Phase II metabolism, *e.g.* glucuronic acid conjugation. We also hypothesized that reduced lipophilicity and larger polar surface (PSA) area would promote renal elimination which would further reduce the risk of DDI. SAR exploration (briefly summarized in Figure 1) revealed that introduction of one or two hydroxy groups in the amine side chains was well tolerated with respect to Kv1.5 potency (and with retained high selectivity vs. hERG and IKs).

- Two secondary amines required
- ≤ 1 cyclic amines (not heterocycles)
- Minimum two of R₁-R₄ must be propyl or larger
- One or two HO or MeO substitution preferred
- Substitution with NH₂, NHMe, MeSO₂ or CONH₂ not tolerated

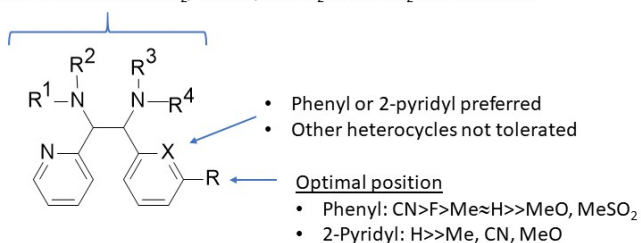


Figure 1. Structure activity relationship (SAR) overview.

As shown in Table 3, glucuronic acid conjugation was indeed observed for compounds **7-10** but disappointingly it represented less than 1.5% of the total metabolism in human hepatocytes (CYP3A4 oxidation still the dominant route). However, the decreased lipophilicity and increased polar surface area, as compared to compound **4**, gave a substantially increased renal elimination in dog, *i.e.* larger fraction in urine for several compounds (**9, 11-14**) and this would contribute to reducing the impact of DDI for patients without renal disease.

As indicated in Table 3, a few compounds were also tested in human atrial myocytes, wherein potency of blockade of the IK_{ur} current was significantly higher than in the CHO cells used for screening. It should be noted here that under our primary assay conditions, the previously mentioned literature compounds BMS-394136 and BMS-919173 showed potency in the same range as our compounds (IC₅₀ = 0.30 μ M and 3.6 μ M respectively, n=2).

Based on an overall assessment of desired properties (potency, dog plasma and renal clearance and alternative routes of elimination), four compounds were chosen for studies of electrophysiological effects in anesthetized rabbits (Table 4). Briefly, increasing doses of test compound were infused intravenously and after 20 minutes, the effective refractory period in the right atrium (RAERP) was measured. The unbound compound plasma exposure which prolonged the RAERP by 20 milliseconds (Ce_{u20}) was predicted by PKPD modelling. An increase of RAERP to such an extent has been suggested to translate into antiarrhythmic efficacy in man¹⁹ and this average exposure was used for early dose to man (eD2M)

predictions which are summarized in Table 4. Based on these data, two compounds, **10** and **12**²⁰, were selected as candidates for studies in a dog disease model.

We have previously reported⁶ that **10** (AZ13395438) caused a concentration dependent and selective increase in atrial refractoriness, with little or no effect on ventricular refractoriness and repolarization or on hemodynamics in the dog. In a rapid atrial pacing (RAP) dog model of AF, **10** converted AF to sinus rhythm in all animals tested (n=12) at an unbound plasma concentration of $0.48 \pm 0.076 \mu$ M.

Guided by these data, **10** emerged as a promising candidate for investigation in the clinical setting. Unfortunately, compound **10**, which can best be characterized as a mixed potassium channel agent, blocking not only Kv1.5 (IC₅₀=1.7 μ M but also Kir3.1/Kir3.44 (I_{KACH}) (IC₅₀=4.1 μ M) and Kv4.3 (IC₅₀=11 μ M),²¹ showed proconvulsant effects in the pentylenetetrazole (PTZ) rat model and produced significant findings in behavioral scoring in the Irwin Screen in the rat.

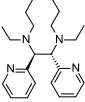
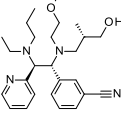
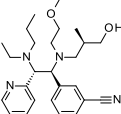
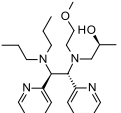
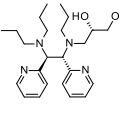
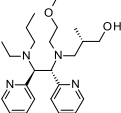
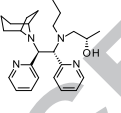
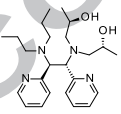
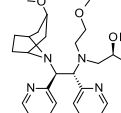
While the mechanisms underlying the observed CNS side effect is not well understood,²² evaluation of additional analogs in the PTZ rat model revealed that the safety margin to predicted human therapeutic exposure was inherently modest (<10 fold) and we therefore stopped working on this lead series and turned our attention to alternative chemical starting points.

The symmetrically substituted chiral compounds **1-4** in Table 1 could be synthesized from the commercially available chiral diamines **15** and **16** using simple alkylation methods (Scheme 1). Whilst compounds **1-3** could be synthesized in one step using 1,5-dibromopentane or propionaldehyde, alkylation of **16** with 1-bromopropane gave selectively the dialkylated compound **17**. A second substituent could then be introduced using reductive amination as exemplified in the synthesis of **4** which is produced *via* aminal **18**. Product formation from the aminal was driven by using excess (> 10 eq) of acetaldehyde and reducing agent that were added in portions during the course of the reaction. Further development leading to a 100 g scale synthesis of enantiomerically pure building block **17** has previously been reported.²³

In addition to the chiral compounds **1-4**, their *meso* forms were also investigated. In this case, the synthesis was performed from *trans* epoxide **19** as described for compound **5** (Scheme 2). The epoxide was synthesized from picolinaldehyde using hexaethylphosphorous triamide, and obtained as a mixture of *cis* and *trans* isomers that was separated using chiral chromatography. Ring opening of *trans* epoxide **19** with piperidine gave amino alcohol **20**, which could be used to introduce a second amine substituent after activation with methane sulfonic anhydride.

By comparing the outcome of the reactions from the *cis* and *trans* epoxides with the products from alkylation of the chiral diamines it became evident that after mesylation of **20** neighboring group participation gives the aziridinium ion **21** as an intermediate. From the epoxide stage to the final product there are therefore three consecutive inversion substitution reactions taking place giving a net inversion of configuration so that the *meso* products are obtained from the *trans* epoxide.

Table 3. Representative compounds illustrating the impact of substitution on potency and PK properties

Compound	Structure	Kv1.5 IC ₅₀ (μ M) ^a	Human atrial myocytes, IKur IC ₅₀ (μ M) ^b	LogD	PSA	Phase II metabolism (glucuronidation) (%) ^c	Dog plasma CL (ml/min/kg)	Dog renal CL (ml/min/kg) ^d
4		3.2 \pm 0.2 (n=3)	Nd	3.3	23	0%	16	0.7 (6.9%)
7 ^e		4.8	0.39 \pm 0.06	2.3	63	1.5%	44	2.1 (4.4%)
8 ^e		7.3	0.26 \pm 0.05	2.4	63	0.5%	37	1.8 (4.7%)
9		2.7 \pm 0.5 (n=4)	Nd	2.7	54	1%	21	2.5 (11%)
10 ^f		1.7	0.06 \pm 0.02	2.6	68	0.5%	6.1	0.19 (5.1%)
11		10	Nd	1.8	54	0%	25	2.7 (11%)
12		3.4	Nd	2.8	45	0%	3.0	0.3 (12%)
13		2.1 \pm 0.3 (n=4)	Nd	2.5	68	0%	16	5.5 (19%)
14		5.6	Nd	2.3	63	0%	25	7.1 (28%)

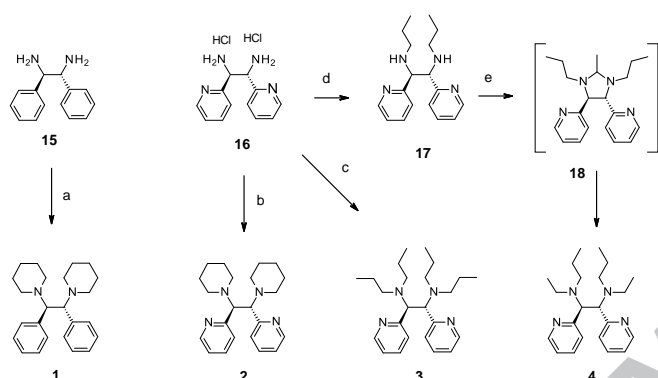
^a n=2 unless otherwise indicated^b n=3 (cells from 1 donor)^c Fraction of the total metabolism that undergoes phase II metabolism (glucuronidation) in human hepatocytes^d Fraction of the dose excreted in urine given in parentheses^e Compounds **7** and **8** are enantiomers. The absolute stereochemistry of the 1,2-diamine has been arbitrarily assigned^f Experimental details including NMR, HRMS and X-ray are summarized in Supplementary material

Table 4.

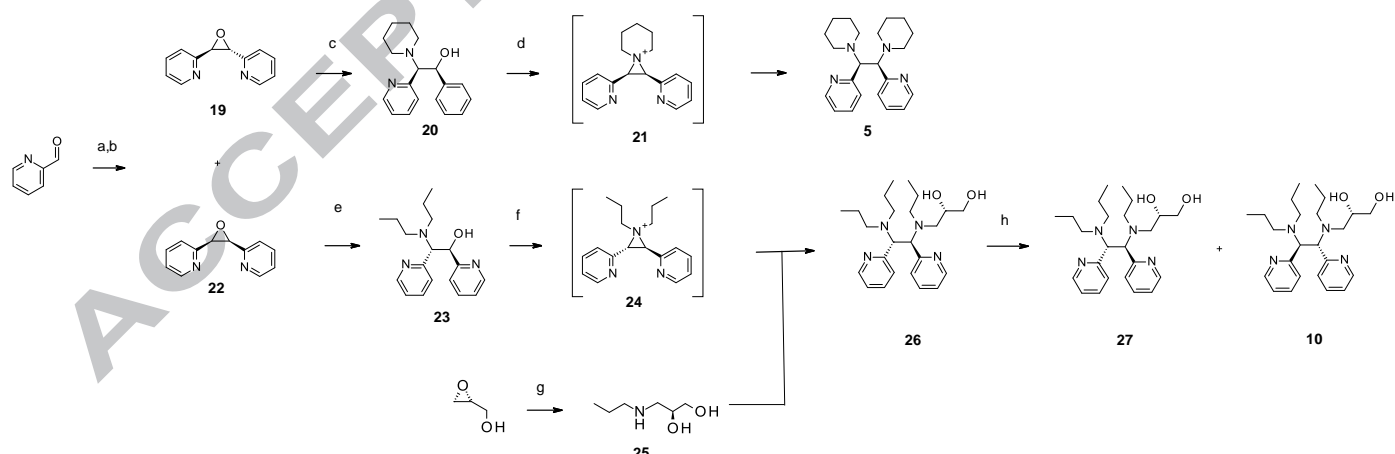
Compound	RAERP Ceu20 (μM) ^a	eD2M (mg/day) ^b
9	0.220	800
10	0.150	700
12	0.057	300
13	0.290	2100

^a Free compound plasma exposure which prolongs the right atrial effective refractory period (RAERP) by 20 ms in the rabbit

^b Estimated dose to man which will give an average free plasma exposure equal to Ceu20



Scheme 1. Reagents and conditions: (a) 1,5-dibromopentane, K_2CO_3 , CH_3CN , rt, 2 days, 85%; (b) 1,5-dibromopentane, Et_3N , DMF, 60 °C, overnight, 63%; (c) propionaldehyde, $\text{NaBH}(\text{OAc})_3$, DCE, rt, 2 days, 29%; (d) 1-bromopropane, Et_3N , DMF, rt, 2 days, 62%; (e) acetaldehyde, $\text{NaBH}(\text{OAc})_3$, DCE, rt, 3 days, 48%.



Scheme 2. Reagents and conditions: (a) hexaethylphosphorous triamide, toluene, -5 °C to rt; (b) chromatography, 32% (19), 23% (22); (c) piperidine, microwave heating, 180 °C, 20 min, used crude; (d) methanesulfonic anhydride, DCM, 0 °C, 30 min, piperidine, rt, 27% (two steps); (e) dipropylamine, IPA, 85 °C, 70 h, 98%; (f) methanesulfonic anhydride, DCM, 0 °C, 4 h, 25, rt, 98%; (g) propan-1-amine, IPA, 70 °C, 2 h, 96%; (h) chiral chromatography separation, 47% (10). The single crystal X-ray structure of compound 10 is shown (data in Supplementary material).

We focused our efforts on the compounds obtained from the *cis* epoxide 22 since those products generally exhibited favorable physicochemical properties in line with what was discussed previously for the symmetrically substituted compounds. As an illustration of the synthetic chemistry used to make non-symmetrically substituted compounds, the synthesis of 10 is described in Scheme 2. The synthetic sequence started from *cis* epoxide 22 that was opened by reaction with the appropriate amine, in this case dipropylamine giving the racemic compound 23. In the next step, a second amine was introduced by activating the amino alcohol 23 with methanesulfonic anhydride giving rise to the intermediate aziridinium ion 24 in analogy with what was previously described. Formation of the aziridinium ion could be monitored by ^1H NMR and when formation was complete, (*S*)-3-(propylamino)propane-1,2-diol 25 was added giving the diastereomeric mixture 26 which was separated by chiral chromatography. Crystallization and X-ray diffraction revealed that 10 has the (*S,S,S*)-configuration as shown in Figure 2.²⁴

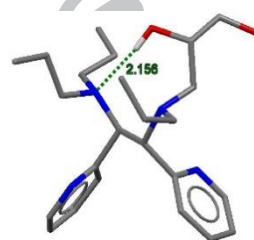


Figure 2. X-ray structure of (*S*)-3-(((1*S*,2*S*)-2-(dipropylamino)-1,2-di(pyridin-2-yl)ethyl)(propyl)amino)propane-1,2-diol (10).

Acknowledgements

The authors would like to acknowledge important scientific contributions from AstraZeneca coworkers Ingemar Jacobsson, Annika Björe, Yantao Chen, Boel Löfgren and Ola Fjellström.

References and notes

- Kirchhof, P.; Benussi, S.; Kotecha, D.; Ahlsson, A.; Atar, D.; Casadei, B.; Castella, M.; Diener, H. C.; Heidbuchel, H.; Hendriks, J.; Hindricks, G.; Manolis, A. S.; Oldgren, J.; Popescu, B. A.; Schotten, U.; Van Putte, B.; Vardas, P. *Eur. Heart J.* **2016**, *37*, 2893.
- Dobrev, D.; Carlsson, L.; Nattel, S. *Nat. Rev. Drug Discov.* **2012**, *11*, 275.
- El-Haou, S.; Ford, J.; Milnes, J. T. *J. Cardiovasc. Pharmacol.* **2015**, *66*, 412.
- Ravens, U. *Can. J. Physiol. Pharmacol.* **2017**, *95*, 1313.
- Walfridsson, H.; Anfinsen, O. G.; Berggren, A.; Frison, L.; Jensen, S.; Linhardt, G.; Nordkam, A. C.; Sundqvist, M.; Carlsson, L. *Europace* **2015**, *17*, 473.
- Jacobson, I.; Duker, G.; Florentzson, M.; Linhardt, G.; Lindhardt, E.; Nordkam, A.; Åstrand, A.; Carlsson, L. *J. Cardiovasc. Pharmacol. Ther.* **2013**, *18*, 290.
- Lloyd, J.; Finlay, H. J.; Vacarro, W.; Hyunh, T.; Kover, A.; Bhandaru, R.; Yan, L.; Atwal, K.; Conder, M. L.; Jenkins-West, T.; Shi, H.; Huang, C.; Li, D.; Sun, H.; Levesque, P. *Bioorg. Med. Chem. Lett.* **2010**, *20*, 1436.
- Gunaga, P.; Lloyd, J.; Mummadi, S.; Banerjee, A.; Dhondi, N. K.; Hennen, J.; Subray, V.; Jayaram, R.; Rajugowda, N.; Reddy, K. U.; Kumaraguru, D.; Mandal, U.; Beldona, D.; Adisechen, A. K.; Yadav, N.; Warriar, J.; Johnson, J. A.; Sale, H.; Putlur, S. P.; Saxena, A.; Chimalakonda, A.; Mandekar, S.; Conder, M.; Xing, D.; Gupta, A. K.; Gupta, A.; Rampulla, R.; Mathur, A.; Levesque, P.; Wexler, R. R.; Finlay, H. J. *J. Med. Chem.* **2017**, *60*, 3795.
- Wolkenberg, S. E.; Nolt, M. B.; Bilodeau, M. T.; Trotter, B. W.; Manley, P. J.; Kett, N. R.; Nanda, K. K.; Wu, Z.; Cato, M. J.; Kane, S. A.; Kiss, L.; Spencer, R. H.; Wang, J.; Lynch, J. J.; Regan, C. P.; Stump, G. L.; Li, B.; White, R.; Yeh, S.; Dinsmore, C. J.; Lindsley, C. W.; Hartman, G. D. *Bioorg. Med. Chem. Lett.* **2017**, *27*, 1062.
- Shunmugam, S. R.; Sugihara, C.; Freemantle, N.; Round, P.; Furniss, S.; Sulke, N. *J. Interv. Card. Electrophysiol.* **2018**, *51*, 191. (The structure of XEN-D0103 has so far not been disclosed.)
- Lagrutta, A.; Wang, J.; Fermini, B.; Salata J. *J. Pharmacol. Exp. Ther.* **2006**, *317*, 1054.
- Olsson, R. I.; Jacobson, I.; Boström, J.; Fex, T.; Björe, A.; Olsson, C.; Sundell, J.; Gran, U.; Öhrn, A.; Nordin, A.; Gyll, J.; Thorstensson, M.; Hayen, A.; Aplanter, K.; Hidestål, O.; Jiang, F.; Linhardt, G.; Forsström, E.; Collins, T.; Sundqvist, M.; Lindhardt, E.; Åstrand, A.; Löfberg, B. *Bioorg. Med. Chem. Lett.* **2013**, *23*, 706.
- Olsson, R. I.; Jacobson, I.; Iliefski, T.; Boström, J.; Davidsson, Ö.; Fjellström, O.; Björe, A.; Olsson, C.; Sundell, J.; Gran, U.; Gyll, J.; Malmberg, J.; Hidestål, O.; Emtenas, H.; Svensson, T.; Yuan, Z.-Q.; Strandlund, G.; Åstrand, A.; Lindhardt, E.; Linhardt, G.; Forsström, E.; Högberg, Å.; Persson, F.; Andersson, B.; Rönnborg, A.; Löfberg, B. *Bioorg. Med. Chem. Lett.* **2014**, *24*, 1269.
- Kajanus, J.; Jacobson, I.; Åstrand, A.; Olsson, R. I.; Gran, U.; Björe, A.; Fjellström, O.; Davidsson, Ö.; Emtenas, H.; Dahlén, A.; Löfberg, B.; Yuan, Z.-Q.; Sundell, J.; Cassel, J.; Gyll, J.; Iliefski, T.; Högberg, Å.; Lindhardt, E.; Malmberg, J. *Bioorg. Med. Chem. Lett.* **2016**, *26*, 2023.
- Boström, J. *ACS Med. Chem. Lett.* **2012**, *3*, 769.
- Schroeder, K.; Neagle, B.; Trezise, D. J.; Worley, J. *J. Biomol. Screen.* **2003**, *8*, 50.
- Wan, H.; Holmén, A. G. *Comb. Chem. High Throughput Screen.* **2009**, *12*, 315.
- Bohnert, T.; Patel, A.; Templeton, I.; Chen, Y.; Lu, C.; Lai, G.; Leung, L.; Tse, S.; Einolf, H. J.; Wang, Y.-H.; Sinz, M.; Stearns, R.; Walsky, R.; Geng, W.; Sudsakorn, S.; Moore, D.; He, L.; Wahlstrom, J.; Keirns, J.; Narayanan, R.; Lang, D.; Yang, X. *Drug. Metab. Dispos.* **2016**, *44*, 1399.
- Finlay, H. J.; Lloyd, J.; Vaccaro, W.; Kover, A.; Yan, L.; Bhawe, G.; Prol, J.; Huynh, T.; Bhandaru, R.; Caringal, Y.; DiMarco, J.; Gan, J.; Harper, T.; Huang, C.; Conder, M. L.; Sun, H.; Levesque, P.; Blonar, M.; Atwal, K.; Wexler, R. *J. Med. Chem.* **2012**, *55*, 3036.
- In high dose PK experiments in dog, **12** showed unwanted ECG effects which may be attributed to stronger blockade of sodium channels as compared to other analogs in the series. No further experiments were carried out with **12**.
- Additional ion channel IC₅₀ data (μM) for **10**: hERG>33μM (37% @ 33μM); IKs>33μM; NaV1.5=19μM; CaV1.2>33μM.
- For **10**, the free brain exposure in rat was ca 4% of the free plasma exposure as determined by measurements of total concentrations in brain and plasma at steady state following a continuous intravenous infusion of **10** at 2μmol/kg/h for a duration of 4h. Free concentrations were then calculated from measured unbound fractions in brain and plasma. Secondary pharmacology profiling offered no clear explanation of the observed effects, but we did observe weak binding to the NMDA receptor (13% and 14% inhibition @ 10μM at the glycine and phencyclidine sites, respectively).
- Karlsson, S.; Lindberg, J.; Sörensen, H. *Org. Process Res. Dev.* **2013**, *17*, 1552.
- Crystal deposition number: CCDC 1881878. In reference 6, the structure of **10** was erroneously assigned as (R,R,S).

Supplementary Material

Experimental procedure for synthesis and X-ray crystallography of compound **10**.